

Article

# Damping of Oscillations of a Rotary Pendulum System

Adam Gavula \* , Peter Hubinský  and Andrej Babinec 

Faculty of Electrical Engineering and Information Technology, Institute of Robotics and Cybernetics, Slovak University of Technology in Bratislava, Ilkovicova 3, 81219 Bratislava, Slovakia; peter.hubinsky@stuba.sk (P.H.); andrej.babinec@stuba.sk (A.B.)

\* Correspondence: adam.gavula@stuba.sk

**Featured Application:** The work described in the paper offers an innovative solution for mitigating unwanted oscillations in rotating systems, such as carousel systems and cranes. This technology has the potential for practical applications in various industries that rely on precise and stable rotational movements. Specific applications could include manufacturing and material handling, but we can also find use in the warehousing and logistics, amusement park rides, robotics and automation, etc.

**Abstract:** This paper describes an innovative design based on the spectral approach of a novel shaper that eliminates frequency components that induce unwanted residual oscillations in various flexible mechanical systems, such as tower cranes or chain carousels, which are vital to many manufacturing and material-handling processes. However, their physical structure leads to flexible effects that limit their usefulness. Apart from the circular motion problem, control is provided by a single actuator, which makes it a so-called underactuated system. The input signal needs to be modified so that the spectral components from several interconnected degrees of freedom are considered together during shaper design, which increases the complexity of this task since one of its components induces nonlinear behavior. This means that traditional shaping techniques, based on linear theory, fail to provide good performance over the whole input range. The underdamped dynamics of the model and the effect of nonlinearities on the spectrum of the final signal are examined; the proposed method for application as a command shaping control technique is applied; and its effectiveness is analyzed by simulation and real-time implementation. The theoretical results verified on an experimental crane system confirm the expected oscillation phenomenon and show that the designed nonlinear shaper can reduce the payload swing significantly.

**Keywords:** input shaping; FIR filter design; swing reduction; motion control; residual vibration control; spectral analysis



**Citation:** Gavula, A.; Hubinský, P.; Babinec, A. Damping of Oscillations of a Rotary Pendulum System. *Appl. Sci.* **2023**, *13*, 11946. <https://doi.org/10.3390/app132111946>

Academic Editor: Luigi Fortuna

Received: 4 September 2023

Revised: 26 October 2023

Accepted: 26 October 2023

Published: 1 November 2023



**Copyright:** © 2023 by the authors. Licensee MDPI, Basel, Switzerland. This article is an open access article distributed under the terms and conditions of the Creative Commons Attribution (CC BY) license (<https://creativecommons.org/licenses/by/4.0/>).

## 1. Introduction

The issue of controlling flexible structures is an extensive area of research, as in many applications, unwanted oscillations are generated due to various elasticities, especially in the case where nowadays there is a demand for the implementation of increasingly faster and more aggressive movements of mechanical systems with flexible elements. Input shaping is a feedforward filtering method that modifies the frequency characteristics of the input signal, thereby reducing the dynamic-motion-induced vibrational response of the system (extracting the input energy around the system's natural frequency). Input shaping schemes first appeared in the 1950s, when early implementations were challenging without digital computers. This method began to be widely applied in the 1980s and 1990s when controlling the movements of various types of cranes by the operator [1–3], which created the need to generate a trajectory in real time, which again limited the number of available algorithms. These methods were often designed for linear movements, and even when

the load moved in different axes (especially in the case of gantry cranes), each could be controlled separately due to multiple actuators.

Sensitivity to modeling errors caused significant residual vibrations [4]. Input shaping became helpful in many natural systems when a robust method was developed [5]. Later, improved methods were introduced to increase robustness further [6]. Due to its robustness, input shaping has been implemented on various systems where precise positioning is required, including robotic manipulators [7], elevators [8], conveyors, throttle control [9], MEMS [10], liquid filling machines [11], etc. While the basic shaping methods assume specific, unchanging characteristics of the system, in the case of various dynamic changes in the system, it is possible to use an extension with adaptive methods, which can also help eliminate nonlinearities [12].

Since the basic principle of shaping techniques is to delay the input signal, this technique can be combined with feedforward control actions, which are crucial to guaranteeing the delay-independent stability of time-delayed systems. Such an integrated approach not only tries to suppress oscillations but also ensures robust stability that takes into account intentional delays caused by shaping techniques and inherent delays of the system, which may also have multiple inputs and outputs [13]. Another possible extension (very popular today), which we also owe to the rapid development of computing technology, is the extension of heuristic methods, which are often based on experience, intuition, or experimental observation and are used to solve problems where a direct and exact calculation can be too complex, difficult, or even impossible. They include various techniques including genetic algorithms [14], neural networks [15–19], PSO algorithms [20,21], and fuzzy [22–24].

The remainder of this paper is structured as follows. Section 2 discusses the time and frequency properties of basic shapers. Section 3 demonstrates the description and simulation of a dynamical system. Section 4 presents a shaper design. The simulation and experimental results, which were performed to verify the proposed design method, are presented in Section 5. The article then ends with pertinent conclusions.

## 2. Input Shaping

Input shaping with time delays is a method of reducing residual vibrations by convolving a sequence of impulses with a baseline reference command to compensate for the undesired oscillatory couple of system poles by the dominant couple of shaper zeros, which ensures a finite settling time for system modes with a known natural frequency and damping ratio. This method can be divided into two categories. In off-line shaping, the trajectory is defined in advance and is constantly repeated during the motion cycle, such as in motor drives used in a printer, hard disks, etc. Suppose we know the trajectory in advance (or at least any initial part), which can be updated in regular cycles. In that case, it is possible to use different forward control (MPC) techniques, which require detailed information about the system and knowledge of the input signal [25,26]. On the other hand, online shaping is a method of preshaping a profile to generate a previously unknown trajectory in which the system is controlled by a human operator or a superior system that acts as a trajectory generator, which means that the input signal needs to be modified in real-time to eliminate spectral components from around the natural frequency.

To demonstrate the basic principle of filtering, we consider the response of a dynamic oscillatory system, which is usually expressed simply by a slightly damped second-order linear transfer function consisting of the estimated values of natural frequency and damping to a series of two pulses, as shown in Figure 1 (red shows the response of the system to the pulses if each was applied individually, and blue shows the combined response of the system resulting from superposition).

This example illustrates that pulses of suitable amplitudes and times can be applied to a system so that the resonant modes of the system are destructively combined, resulting in the minimization of the resulting vector component pulses. The FIR shaper structure can be expressed by a series of Dirac pulses, where  $D_i$  represents the time course of the Dirac pulse. Each of the pulses is assigned the corresponding amplitude  $A_i$  for the time delay

$T_{Dn}$  of the ( $n$ th) Dirac pulse relative to the first of the series, for which we assume a delay with a zero value (Figure 2).

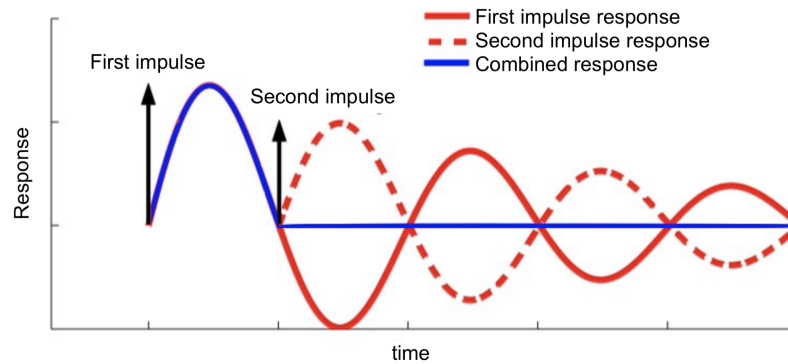


Figure 1. System response to a single and combined impulse.

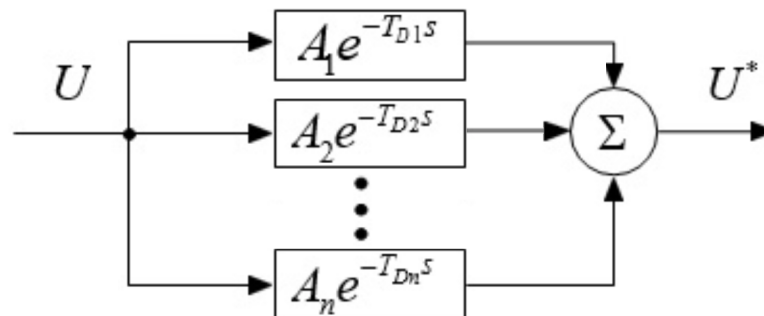


Figure 2. The internal structure of the ( $n$ th) order shaper.

From a mathematical point of view, the transition of the signal through a parallel combination of transport delays can therefore be replaced by the operation of convolutional multiplication of the reference signal with a sequence of Dirac pulses, which means that the control signal will be decomposed into several time-shifted components, which will individually excite sub-oscillations. However, these oscillations are attenuated in sum due to appropriately set phase shifts and amplitudes. This process requires one multiplication and one addition operation for each pulse. The basic block diagram of the molding principle is shown in Figure 3.

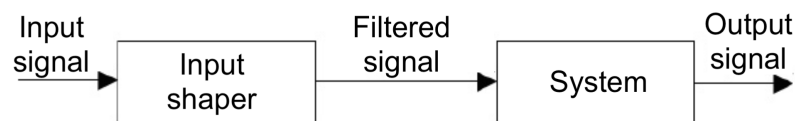


Figure 3. Block diagram of the system with input shaper.

Since the input shaper must be placed directly in front of the time-varying controlled system, there is no feedback to help set the control signal correctly [5,27]. By identifying the output of the controlled system, it is possible to correctly configure the input shaper and then modify the control signal in the desired way.

### 2.1. Shaper Constraints

Due to the transcendental nature of the problem, there can be an infinite number of solutions. To choose a practical solution, it is necessary to define a set of different limiting equations (conditions), which are based on requirements, by which it is possible to determine the amplitudes and temporal positions of the pulses of the input shaper [28,29]. One of the fundamental limitations is the limitation of pulse amplitudes. If the pulse amplitudes are not limited, their values can reach positive or negative infinity due to time optimality [30]. The solution to this problem may be to limit the size of the pulses or require

that all pulses have positive values. Limiting the pulse amplitudes is also necessary to ensure that the shaped input signal reaches the same final steady-state value as the original reference signal without shaping. This limitation is not explicitly stated in some filtered algorithm designs (especially in those where the filter has a non-linear character). It is often solved in an iterative way [31]. To prevent a change in the size of the control pulse, the sum of all amplitudes must equal one. The next limitation, perhaps the most important, is the condition for limiting residual vibrations (it was mentioned earlier as a vector condition). In many publications, this condition is associated with a dimensionless quantity of residual vibration amplitude, or the percentage ratio of vibrations (PRV) with input shaping to vibrations without input shaping. The mentioned ratio of amplitudes can be expressed as a function of the natural frequency,  $\omega$ , and the damping coefficient,  $b$ , of the system, which can be written in the form of an equation prescribing the zero value of the amplitude of the vector sum of all Dirac pulses forming the relevant type of shaper.

The limitations mentioned so far are sufficient for the design of the basic (early) shaper (ZV), which has a very symmetrical structure (two appropriately shifted pulses in time), as demonstrated in Figure 1. The first impulse can be applied almost immediately (which is mainly desired). However, the second pulse is shifted in time by half of the oscillation period, which in most applications has proven to be a sufficient settling time but is directly related to the system frequency, which means that in the case of low-frequency dynamics, a high delay can occur.

In reality, it is not possible to model this entirely accurately, or identify the parameters. Therefore, robustness to modeling errors is one of the other important factors. Suppose that small changes occur in the system, either due to inaccurate identification or in the case of a change in the length of the rope, the weight of the load, or any other property that can fundamentally affect the system parameters (mainly the frequency). In that case, the set parameters of this shaper will no longer be able to remove oscillations for the system, and with these changes, the residual oscillations will increase proportionally. Therefore, it is necessary to introduce another condition related to robustness. While the ZV shaper will theoretically provide zero vibration at the modeling frequency, it is sensitive to modeling errors [32]. This sensitivity makes the ZV shaper impossible to use practically on many systems.

The robustness of input shapers is most commonly graphically represented by sensitivity curves. These curves show the percentage of residual vibration against the normalized vibration frequency. Insensitivity is one of the key measures of robustness derived from the sensitivity curve [6,33]. Insensitivity is the width of the sensitivity curve at the tolerated percentage level ( $V_{TOL}$ ) with respect to the monitored parameter. Generally, the more robust the shaper is, the more it can handle damping in the event of nonlinearities. Singer and Seering were the first to develop an input shaping technique with an extended region around the system's natural frequency, which is robust enough to be used in most cases. To reduce the sensitivity of the input shaper to natural frequency errors, the shaper must meet another constraint, which consists of setting the derivative of the vibration equation with respect to the natural frequency to zero at the modeling frequency (ZVD). Limiting the zero derivative places additional zeros on the flexible poles, flattening the sensitivity curve at the modeled frequency and increasing insensitivity. This shaper has one pulse more, and the time lead equals one period of the vibration frequency. This shaper is based on ZV, and we paid for the increase in robustness by increasing the transition time of the system, which means that input shaping has a fundamental compromise between robustness and the duration of the shaper. An input shaper with even greater insensitivity than the ZVD shaper can be obtained by setting the second derivative to zero. This shaper is called the ZVDD shaper [34]. We could thus modify the algorithm by using an indefinitely repeated derivation of the vibration percentage equation (ZVDDD...). For each derivative, an additional pulse is added to the shaper. Thus, the shaper is extended by half the frequency period.

It is generally proven that in real systems, a particular modeling error will occur, so it is not advisable to try to get the vibrations around the natural frequency to zero, but rather to limit the vibrations to a certain low but at the same time acceptable level [6]. The extra-insensitive shaper extends the robustness of the ZVD shaper. When modeling this type of shaper, the constant  $V_{TOL}$  is given, which is generally equal to the upper limit of the acceptable residual oscillations, and thus, with an increase in the allowed size of oscillations, the insensitivity to modeling errors increases. The EI shaper has the exact same pulse times as the ZVD shaper but with different amplitude values, resulting in greater robustness. Like zero-derivative methods, this idea can be extended from a basic shaper with a single hump in the sensitivity curve to a higher level of robustness by adding constraints that create multiple humps in the curve, called Multi-Hump EI Shapers.

Given the wide variety of systems that can benefit from input shaping, it seems desirable to develop a shaping method that specifies insensitivity and tailors the shaper's robustness to the specific system for which it may be designed. There are several ways to design this type of shaper, for example, using an approximation method where the vibrations are limited below a certain tolerable level at several points in the range of the required parameters, but this method provides approximate solutions. The amplitudes and times of the shaping pulses are then generated using optimization procedures. In practice, it is possible to use a small number of points to suppress vibrations in a wide range of parameters. The second procedure is more challenging to implement but brings accurate solutions. The advantage is that they can be designed to have non-symmetrical sensitivity curves so that the shaper is more robust and resistant to frequency increases than frequency decreases or vice versa. One disadvantage of the SI shaper is that optimization is required [35,36].

An alternative limitation for constraints on time optimality allows the pulses to acquire negative but finite values, which causes a reduction in the time of individual pulses and thereby speeds up the entire process of ramping up to the desired value of the control pulse. With this type of shaper (UMZV), one can expect favorable properties concerning the overall delay, but at the expense of less robustness and possible high-mode excitation. Significant distinctions can be made between input-shaped commands and smooth commands based on their shape, design approach, and system response. The previous concepts cannot be used if a distributed delay is needed because they have a lumped delay [37,38]. As part of the design, it is necessary to determine the interval and the parameter  $D$  based on a spectral analysis. In most cases, smooth profiles have the effect of a low-pass filter, while input shaping is similar to a notch filter. Previous papers have indicated that shaped commands move systems faster than smooth commands [39]. The combination of three Dirac pulses with the same amplitude is another type of shaper that belongs to the group of faster shapers. The total delay of the shaper's approach to the desired value of the control pulse is two-thirds of the system's natural frequency period. This type of shaper represents a compromise between speed and the robustness of input signal shaping. If we continued to increase the impulses gradually, we would observe a decrease in the steepness of the course in the vicinity of the spectrum of the system's angular frequency. However, this reduction would be accompanied by a gradual increase in the total value delay of the shaper up to the value  $T_D$  when the signal at the output of the shaper would pass into a trapezoidal waveform with the length of the edges  $T_D$  [40].

## 2.2. Input Shaping for Multiple Vibration Modes

There are also ways to use input shaping to reduce vibration in multiple modes. One way is to design shapers for each oscillation mode and combine them [41,42]. The resulting shaper will minimize vibration at the desired frequencies, with added robustness for higher-mode excitation. Another way to design a shaper is to solve the constraint equations for the two modes simultaneously [43,44]. This method reduces vibrations near the modeling frequencies but does not suppress high-vibration modes as much. If the second pair of oscillating poles still causes an unacceptable vibration level, adding a second filter for the

faster poles and connecting it in series with the first one is possible. To solve the problem of multiple vibration modes, it is also possible to use the previously mentioned adaptive methods [45]. Another possible solution to the problem of multiple vibration modes is a solution based on the zero-placement nominal mode technique, which means that all modes are placed in the allowed range (two EI shapers) [46].

### 3. Problem Formulation and System Description

A dynamic system can be determined by modeling the system using the equations of motion and then solving for the Laplace or Fourier transform of the output in terms of the input. The transfer function of a rotary pendulum system is a mathematical representation of the system’s behavior. It describes the relationship between the input (angular acceleration of the carousel) and the output (angular position of the load). A damped oscillatory system is mainly expressed by a second-order linear transfer function, which consists of estimated values of the natural frequency,  $\omega$ , and damping,  $b$ . In this case, we consider the linearization of the pendulum model for small deflection values [47,48] and a rope that is solid, inelastic, and not subject to any twisting, friction, or other non-ideal properties. On the contrary, we do not assume any other oscillating modes given by the flexibilities of the arm, column, etc. The dynamics of a gantry crane usually consist of two interconnected parts that represent the oscillation of the load in each axis.

The dynamics of the motor can affect the dynamic properties, but if the dynamics of the motor (response) are faster than the dynamics of the load, there is no significant influence on the position of zeros in the transfer function of the system. Then, the motor should be able to effectively control the load without significantly changing the dynamic characteristics of the overall system. Its contribution to the overall system’s response can only be in the rounding of the waveforms, which means that the response is smoother, and thus the motor is unlikely to be a limiting factor in controlling the system’s response. If the bandwidth of the motor servo is much higher than the natural frequency of the load, it means that the motor responds quickly to changes in the control signal, which will ensure fast and accurate control of the load. The dynamics of the actuators (also current loop, etc.) can be defined by a first-order transfer function with a low time constant, but it is omitted because the electrical time constant of the actuator is negligible compared to the mechanical time constant of the entire system.

The subject of the analysis in this article is a rotating carousel system, which consists of a fixed structure and arms that rotate around the axis of the vertical structure. Both arms have oscillating rope-suspended loads that exhibit low damping properties. A similar mechanism is the rotary pendulum, which has several basic similarities with the described system. The chain carousel rotates at a prescribed angular velocity about a vertical axis, while the loads move in several degrees of freedom that are coupled. The dynamics of these systems are usually characterized by significant feedforward nonlinearities, nonholonomic constraints, a non-minimum phase, and underactuated dynamics. A chain carousel model with a diameter of 62 cm and a rope length of 22 cm in the Cartesian plane is shown in Figure 4.

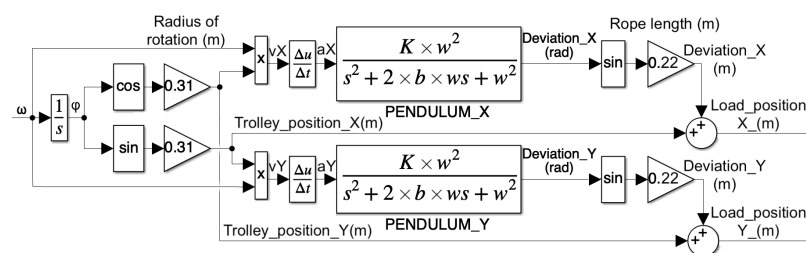


Figure 4. Block diagram of the carousel model in Cartesian coordinates.

This case is interesting because two different accelerations controlled by one motor affect the deflection of the load relative to the stable position. One acceleration is the tangential acceleration proportional to the angular acceleration, which we directly influence by controlling the torque of the motor driving the mechanism.

$$a_{tang} = r \times \epsilon = r \times \frac{d\omega}{dt} \tag{1}$$

The second acceleration is the centrifugal acceleration, which is proportional to the square of the angular velocity of the load.

$$a_{rad} = r \times \omega^2 \tag{2}$$

The resulting acceleration amplitude acting on the hinge is

$$\sqrt{ax^2 + ay^2} = \sqrt{a_{rad}^2 + a_{tang}^2} \tag{3}$$

This acceleration turns with the motion of the arm. The resulting block diagram in Figure 5 represents an intuitive principle model from the distribution point of view, split into tangential and radial components.

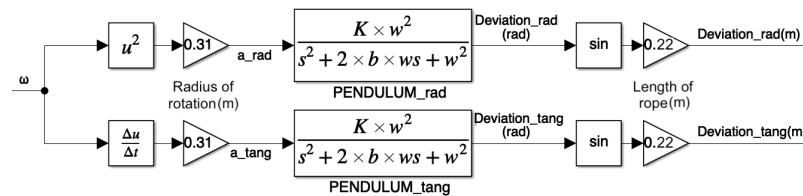


Figure 5. Block diagram of the carousel model in polar coordinates.

Since the pendulum is attached to the rotating frame like a carousel, during the braking maneuver, the coordinate system of the pendulum does not coincide with the coordinate system of the arm due to torsional but also Coriolis and other forces. We also consider a torsionally freely rotating rope whose torsional force is insufficient for the load, which means that in addition to the linearization of the pendulum, we also consider the linearization of the system by ensuring that the carousel does not turn too much of an angle during the braking maneuver.

#### 4. Shaper Design

In most cases, the fixed shaper is designed, based on a linearized version, around the operating point of the nonlinear system, which causes linear behavior (when the payload swing angles are relatively small). By eliminating the corresponding component of the spectrum in the angular acceleration signal, we will simultaneously eliminate this part of the spectrum in the angular velocity signal as well (since the zeros in the velocity spectrum are the same as the zeros in the acceleration spectrum but divided by the velocity itself). Typically, the shaper is designed for shaping the acceleration spectrum. In applying the structure according to Figure 6, when we eliminate the relevant spectrum components in the angular acceleration (velocity) control signal, we can successfully suppress oscillations in the tangential direction [40].

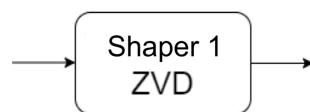


Figure 6. Structure of linear shaper.

Based on the relations derived in Section 3, (1)–(3), it is clear that it is also necessary to shape the spectrum of the square of the angular velocity, which is proportional to the centrifugal acceleration. At large angular velocity values, oscillations can also occur in the radial direction due to the action of centrifugal forces, which causes a non-linear effect. As a result, the spectrum of the input signal is distorted, and the problem of shaping is more complex in this case. If we apply the scheme according to Figure 7, it is possible to suppress oscillations in the radial direction and vice versa, so oscillations in the tangential direction will appear [40].



Figure 7. Structure of non-linear shaper.

One of the possible solutions to effectively eliminate oscillations in both axes and remove the second component of the oscillation is to connect a series shaper extended by nonlinearity (Figure 8) [40].

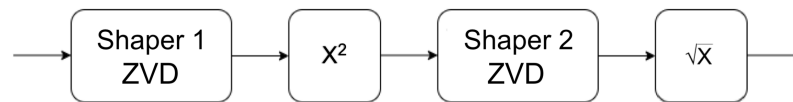


Figure 8. Structure of combined shaper.

This combined filter gives the square root in the branch for centrifugal acceleration, which linearizes the given term, but to shape the spectrum correctly, the square root must be given in front of the shaper [40].

### 5. Verification of the Method

#### 5.1. Simulation Verification

This section conducted simulations based on the Matlab software (version number for MATLAB is 9.12.0.1884302 (R2022a)) simulation platform to verify the proposed method. Figure 9 shows the resulting motion of the simulated load in the Cartesian system for the unshaped (red) case and for the linear (green), non-linear (blue), and combined (black) ZVD shapers.

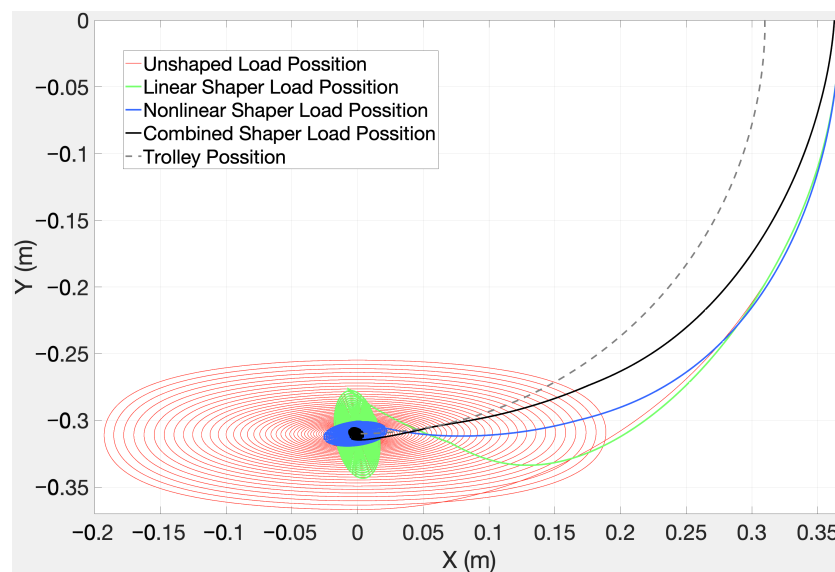
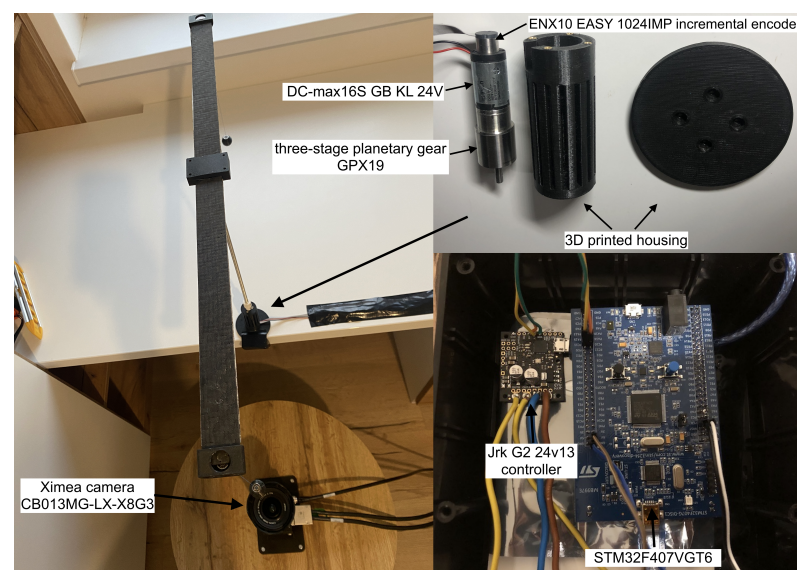


Figure 9. Simulated load and trolley trajectories for the unshaped and shaped case.

It can be seen from the resulting simulations that the radial component remains with the linear shaper and the tangential component remains with the non-linear shaper. In the case of a linear shaper, there is a ten-fold attenuation in the tangential direction and twice as much in the radial direction. In the case of a non-linear shaper, the direct component is equally damped, and in the radial direction there is a six-fold attenuation. In the case of the combined shaper, the tangential component is damped thirty times and the radial component twelve times compared to the unshaped case. It is also possible to notice that the trajectories are not curved due to the torsional (Coriolis, etc.) force during the end of the input pulse.

### 5.2. Real-System Verification

Among the next steps in verifying the shaping methods is the realization of experiments on a reduced carousel model, which is shown in Figure 10. The dimensions of the real model are the same as those considered in the simulation.



**Figure 10.** The experimental carousel system.

A brushed DC-max16S GB KL 24V motor from Maxon company Maxon Motor AG, located in Sachseln, Switzerland, controls the slew motions. It is possible to control the speed or position of the motor based on a signal from the ENX10 EASY 1024IMP incremental encoder. On the other side of the shaft is a three-stage planetary gear GPX19 with a gear ratio of 186:1. This motor is connected to the Jrk G2 24v13 controller, which generates the required PWM properties based on commands from serial communication with the microcontroller STM32F407VGT6. A threaded rod with a diameter of 6 mm is connected to the motor shaft, which serves as a vertical segment and forms the central support of the entire carousel structure. The top of the carousel is made of a laminated carbon fiber strip attached to a vertical bar. This belt is the mounting point for the pendulums, which are connected by rope to bearings that help dampen the effect of the torsion force. All mounts, couplings, and loads are 3D printed. Another aspect of this setup is how we sense this motion. A high-frame-rate CB013MG-LX-X8G3 camera from Ximea company Ximea GmbH, located in Münster, Germany, is located at the bottom of the device, which sense the pendulum's movement from below. Using optical flow technology and the OpenCV library, the camera captures oscillations, which makes it possible to identify the presented system with sufficient quality.

## 6. Results

During the realization of the experiments, the crane started rotation and rotated at the same speed (26 rpm) until the oscillations generated by the acceleration stabilized. Experiments with various changes in the testing paradigm (load changes) were also performed. The first load weighs 1.5 g (Figure 11), the second one weighs five times this, that is, 7.5 g (Figure 12), and the third one weighs 10 times the original, so 15 g (Figure 13). Since this article deals with the analysis of finite impulses, we are mainly interested in the moment when the crane receives the command to stop. The figure shows the trajectory of the load in the unshaped (red), linear (green), non-linear (blue), and combined (black) cases. Each resulting load movement is smoothed using a Savitzky–Golay filter [49].

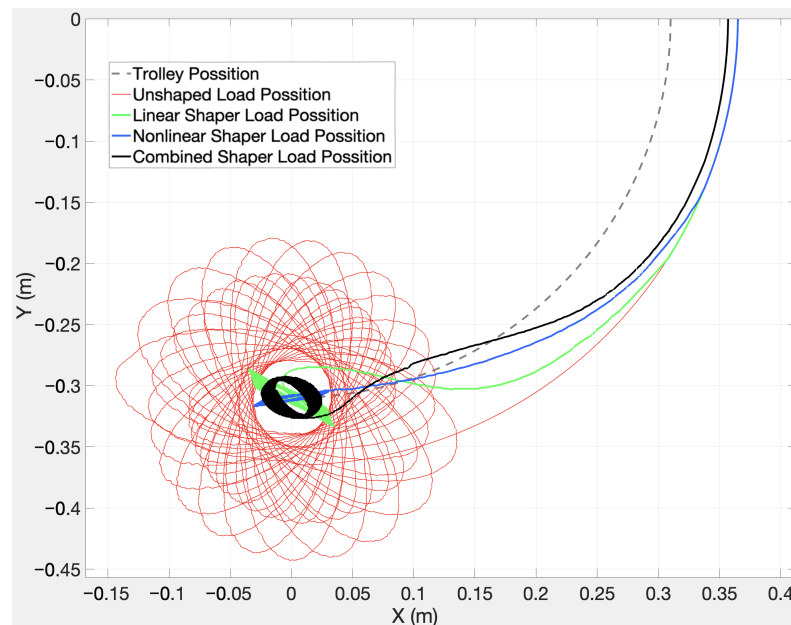


Figure 11. Experimental load (1.5 g) and trolley trajectories for the unshaped and shaped case.

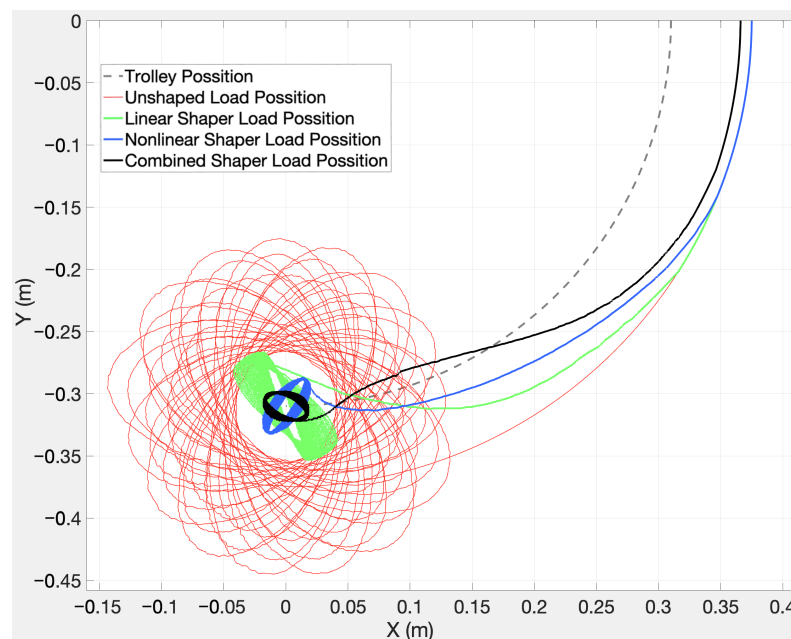
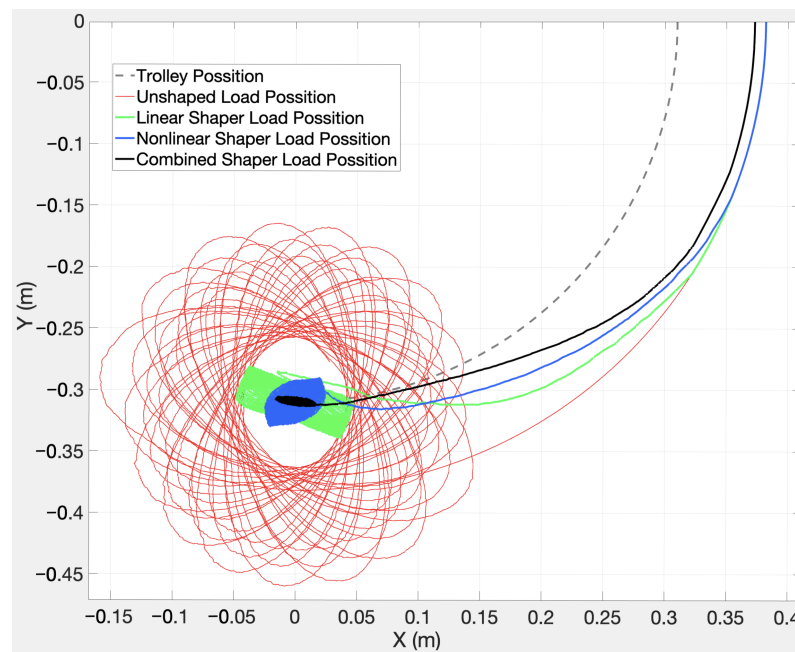


Figure 12. Experimental load (7.5 g) and trolley trajectories for the unshaped and shaped case.



**Figure 13.** Experimental load (15 g) and trolley trajectories for the unshaped and shaped case.

## 7. Discussion

The resulting waveforms from the experiments on the real model clearly confirmed the predicted behavior, which turned out to be identical to the simulated trajectories. The perpendicularity of these two components is also clearly visible. In the case of using a linear shaper, there was an almost six-fold attenuation in the tangential direction and three-fold in the radial direction. The non-linear shaper damps the tangential component three times and the radial component six times. Depending on the weight of the load, there is more dampening. In the case of the combined shaper, there is a six-fold attenuation in both directions, but in the case of a greater weight, it is more.

Due to the not very significant changes in the results of the experiments with different weights of loads, the theory of the immaterial suspension, which is basically a mathematical pendulum where the period of oscillations does not depend on the weight of the load, was confirmed.

Compared to the simulation, the bending of the plane in which the load oscillates due to the twisting of the hanging rope is visible. In the case of shaped courses, this rolling is not so pronounced. By using bearings, we managed to eliminate the effect of the torsional force to a certain extent.

It is also important to mention the limitations of our approach. Although the combined filter shows a significant improvement over the linear or non-linear filter, its effectiveness may be limited at higher angular velocities. Due to the fact that there are limits regarding the rotation angle of the carousel during the braking maneuver, it is important to remember that in the case of turning by 180 degrees, opposite oscillations can be induced, which greatly impairs the effectiveness of the proposed algorithm. The solution to this problem would be the use of a shorter shaper, for example, UMZV, which would minimize the size of the turn during the braking maneuver. Therefore, it would be worthwhile to investigate how effective these algorithms are at higher speeds.

From the point of view of safety, it is also important that there is no greater displacement of the stopping point compared to the space where oscillations occur in the unformed case. In our case, we chose the speed limit.

## 8. Conclusions

In this paper, based on system analyses, we designed and implemented an innovative shaper, which, based on various experiments, successfully suppresses those frequency

components that generate oscillations in rotating systems such as carousel systems or cranes. Such systems are usually driven by one drive, while it is necessary to simultaneously eliminate oscillations in different directions. In each of them, oscillations occur for different reasons, which represents a non-linear problem. It is clearly demonstrated that the combined filter, which takes into account the complexity of the input signal, provides significantly better results in limiting load oscillations during the braking maneuver compared to an unshaped, linear, or non-linear filter alone.

When we look at previous studies in this area, many of them mostly focused on the use of linear filters, but less focused on nonlinear or combined approaches. Our work brings a new dimension by showing that integrated solutions can be more effective than individual components. This gives us evidence of the limitations of linear methods and shows the need to develop methods that take nonlinear effects into account. The same problem is solved in another paper [50], where the problem is analyzed in a similar way, but the solution is difficult to calculate and use.

It is also important to emphasize that even though our results show the positive effects of the combined filter, there are still possibilities for its further optimization. Further investigation is also needed in the context of the mentioned high angular speed of rotation.

The use of such approaches can also be applied in the case of more complex systems, such as mobile chassis that move in a warehouse environment, where there is a requirement for the fastest possible movements while scanning various barcodes or QR codes using a camera. Due to oscillations during movement, it is necessary to wait until the image stabilizes and focuses so that the images are sharp. Such a system can, in addition to forward and backward movement, move along a circular trajectory, which represents a similar issue to the carousel investigation case. Therefore, in addition to investigating time-optimal solutions, our future research will also focus on applications for other systems.

**Author Contributions:** Conceptualization, P.H. and A.G.; methodology, P.H.; software, A.G.; validation, A.G.; formal analysis, P.H. and A.G.; investigation, P.H. and A.G.; resources, P.H. and A.G.; data curation, A.G.; writing—original draft preparation, A.G.; writing—review and editing, P.H. and A.G.; visualization, A.G.; supervision, P.H.; project administration, P.H.; funding acquisition, A.B. All authors have read and agreed to the published version of the manuscript.

**Funding:** The authors gratefully acknowledge the contribution of the Scientific Grant Agency of the Slovak Republic under the grant 1/0049/20 and the Program for the Support of Young Researchers (project with contract 1348).

**Institutional Review Board Statement:** Not applicable.

**Informed Consent Statement:** Not applicable.

**Data Availability Statement:** The data presented in this paper are available at <https://drive.google.com/drive/folders/1pOqxhiKmcLUtG-D1lu5SUyjMcxEcKXdW?usp=sharing>, accessed on 31 October 2023.

**Conflicts of Interest:** The authors declare no conflict of interest.

## References

1. Calvert, J.F.; Gimpel, D.J. Method and Apparatus for Control of System Output in Response to System Input. U.S. Patent, No. 2,801,351, 30 July 1957.
2. Smith, O.J.M. Posicast control of damped oscillatory systems. *Proc. IRE* **1957**, *45*, 1249–1255. [[CrossRef](#)]
3. Smith, O. *Feedback Control Systems*; McGrawHill Book Co., Inc.: New York, NY, USA, 1958.
4. Drapeau, V.; Wang, D. Verification of a closed-loop shaped-input controller for a five-bar-linkage manipulator. In Proceedings of the IEEE International Conference on Robotics and Automation, Atlanta, GA, USA, 2–6 May 1993.
5. Singer, N.C.; Seering, W.P. Preshaping Command Inputs to Reduce System Vibration. *J. Dyn. Sys. Meas. Control* **1990**, *112*, 76–82. [[CrossRef](#)]
6. Singhose, W.; Seering, W.; Singer, N. Residual vibration reduction using vector diagrams to generate shaped inputs. *J. Mech. Des.* **1994**, *116*, 654–659. [[CrossRef](#)]
7. Magee, D.P.; Book, W.J. Filtering Micro-Manipulator Wrist Commands to Prevent Flexible Base Motion. In Proceedings of the Proceedings of American Control Conference, Seattle, WA, USA, 21–23 June 1995.

8. Fortgang, J.; Patrangenaru, V.; Singhose, W. Scheduling of input shaping and transient vibration absorbers for high-rise elevators. In Proceedings of the American Control Conference, Minneapolis, MN, USA, 14–16 June 2006; p. 6.
9. Park, K.; Lee, J.; Park, J. Torque control of a vehicle with electronic throttle control using an input shaping method. *Int. J. Automot. Technol.* **2013**, *14*, 189–194. [[CrossRef](#)]
10. Daqaq, M.F.; Reddy, C.K.; Nayfeh, A.H. Input-shaping control of nonlinear MEMS. *Nonlinear Dyn.* **2008**, *54*, 167–179. [[CrossRef](#)]
11. Pospiech, T.; Hubinský, P. Input shaping for slosh-free moving containers with liquid. *Int. J. Mech. Control* **2009**, *9*, 13–20.
12. Stergiopoulos, J.; Tzes, A. Adaptive input shaping for nonlinear systems: A case study. *J. Dyn. Sys. Meas. Control* **2007**, *129*, 219–223. [[CrossRef](#)]
13. Bucolo, M.; Buscarino, A.; Fortuna, L.; Frasca, M. Forward Action to Stabilize multiple Time-Delays MIMO Systems. *Int. J. Dyn. Control* **2023**, *1*, 1–9. [[CrossRef](#)]
14. Duong, Q.K.; Chovanec, L.; Hubinsky, P.; Vozak, D.; Matuga, M.; Varga, P. Comparison of input shaper based on genetic algorithms with analytical approach. *Int. J. Artif. Intell.* **2017**, *15*, 21–32.
15. Duong, S.C.; Uezato, E.; Kinjo, H.; Yamamoto, T. A hybrid evolutionary algorithm for recurrent neural network control of a three-dimensional tower crane. *Autom. Constr.* **2012**, *23*, 55–63. [[CrossRef](#)]
16. Ramli, L.; Mohamed, Z.; Jaafar, H.I. A neural network-based input shaping for swing suppression of an overhead crane under payload hoisting and mass variations. *Mech. Syst. Signal Process.* **2018**, *107*, 484–501. [[CrossRef](#)]
17. Moreno, L.; Acosta, L.; Méndez, J.A.; Torres, S.; Hamilton, A.; Marichal, G.N. A self-tuning neuromorphic controller: Application to the crane problem. *Control Eng. Pract.* **1998**, *6*, 1475–1483. [[CrossRef](#)]
18. Méndez, J.A.; Acosta, L.; Moreno, L.; Torres, S.; Marichal, G.N. An application of a neural self-tuning controller to an overhead crane. *Neural Comput. Appl.* **1999**, *8*, 143–150. [[CrossRef](#)]
19. Toxqui, R.; Yu, W.; Li, X. Anti-swing control for overhead crane with neural compensation. In Proceedings of the IEEE International Joint Conference on Neural Network, Vancouver, BC, Canada, 16–21 July 2006.
20. Maghsoudi, M.J.; Mohamed, Z.; Sudin, S.; Buyamin, S.; Jaafar, H.I.; Ahmad, S.M. An improved input shaping design for an efficient sway control of a nonlinear 3D overhead crane with friction. *Mech. Syst. Signal Process.* **2017**, *92*, 364–378. [[CrossRef](#)]
21. de Moura Oliveira, P.B.; Solteiro Pires, E.J.; Boaventura Cunha, J. Particle swarm optimization for gantry control: A teaching experiment. In Proceedings of the 15th Portuguese Conference on Artificial Intelligence—EPIA 2011, Lisbon, Portugal, 10–13 October 2011; Springer: Berlin/Heidelberg, Germany, 2011; Volume 15.
22. Smoczek, J. Fuzzy crane control with sensorless payload deflection feedback for vibration reduction. *Mech. Syst. Signal Process.* **2014**, *46*, 70–81. [[CrossRef](#)]
23. Chang, C.-Y. Adaptive fuzzy controller of the overhead cranes with nonlinear disturbance. *IEEE Trans. Ind. Inform.* **2007**, *3*, 164–172. [[CrossRef](#)]
24. Solihin, M.; Iwan, M.; Wahyudi; Legowo, A. Fuzzy-tuned PID anti-swing control of automatic gantry crane. *J. Vib. Control* **2010**, *16*, 127–145. [[CrossRef](#)]
25. Giacomelli, M.; Faroni, M.; Gorni, D.; Marini, A.; Simoni, L.; Visioli, A. Model predictive control for operator-in-the-loop overhead cranes. In Proceedings of the IEEE 23rd International Conference on Emerging Technologies and Factory Automation (ETFA), Turin, Italy, 4–7 September 2018; Volume 1.
26. Schaper, U.; Arnold, E.; Sawodny, O.; Schneider, K. Constrained real-time model-predictive reference trajectory planning for rotary cranes. In Proceedings of the IEEE/ASME International Conference on Advanced Intelligent Mechatronics, Wollongong, Australia, 9–12 July 2013.
27. Murphy, B.R.; Watanabe, I. Digital shaping filters for reducing machine vibration. *IEEE Trans. Robot. Autom.* **1992**, *8*, 285–289. [[CrossRef](#)]
28. Pereira, E.; Trapero, J.R.; Díaz, I.M.; Feliu, V. Adaptive input shaping for manoeuvring flexible structures using an algebraic identification technique. *Automatica* **2009**, *45*, 1046–1051. [[CrossRef](#)]
29. Pereira, E.; Trapero, J.; Diaz, I.; Feliu, V.; Robertson, M.; Kozak, K.; Singhose, W. Computational framework for digital input shapers using linear optimisation. *IET Control Theory Appl.* **2006**, *153*, 314–322.
30. Singer, N.C. *Residual Vibration Reduction in Computer Controlled Machines*; Technical Report Number AITR-1030; MIT Artificial Intelligence Lab: Cambridge, MA, USA, 1989.
31. Mavroidis, C.; Antoniadis, I.; Lee, C. Maximally robust input preconditioning for residual vibration suppression using low-pass fir digital filters. *J. Dynam. Syst. Meas. Control* **2002**, *124*, 85–97.
32. Tallman, G.; Smith, O. Analog study of dead-beat posicast control. *IRE Trans. Autom. Control* **1958**, *4*, 14–21. [[CrossRef](#)]
33. Singhose, W.E.; Seering, W.P.; Singer, N.C. Shaping inputs to reduce vibration: A vector diagram approach. In Proceedings of the IEEE International Conference on Robotics and Automation, Cincinnati, OH, USA, 13–18 May 1990; pp. 922–927.
34. Vaughan, J.; Yano, A.; Singhose, W. Comparison of robust input shapers. *J. Sound Vib.* **2008**, *315*, 797–815. [[CrossRef](#)]
35. Singhose, W.E.; Seering, W.P.; Singer, N.C. Input shaping for vibration reduction with specified insensitivity to modeling errors. In Proceedings of the Japan-USA Symposium on Flexible Automation, Boston, MA, USA, 7–10 July 1996; Volume 1, pp. 307–313.
36. Singer, N.C.; Seering, W.P. An Extension of Command Shaping Methods for Controlling Residual Vibration Using Frequency Sampling. In Proceedings of the IEEE International Conference on Robotics and Automation, Nice, France, 12–14 May 1992; Volume 1, pp. 800–805.

37. Vyhliđal, T.; Kučera, V.; Hromčık, M. Signal shaper with a distributed delay: Spectral analysis and design. *Automatica* **2013**, *49*, 3484–3489. [[CrossRef](#)]
38. Maghsoudi, M.J.; Mohamed, Z.; Tokhi, M.O.; Husain, A.R.; Abidin, M.S.Z. Control of a gantry crane using input-shaping schemes with distributed delay. *Trans. Inst. Meas. Control* **2017**, *39*, 361–370. [[CrossRef](#)]
39. Eloundou, R.; Singhose, W. Justification for using step-function reference commands: Comparison to S-curves. *IFAC Proc. Vol.* **2002**, *35*, 25–30. [[CrossRef](#)]
40. Hubinský, P. *Riadenie Mechatronických Systémov s Nízky m Tlmením*, 1st ed.; STU: Bratislava, Slovakia, 2010; ISBN 9788022733106.
41. Hyde, J.M.; Seering, W.P. *Using Input Command Pre-Shaping to Suppress Multiple Mode Vibration*; MIT Space Engineering Research Center: Cambridge, MA, USA, 1990.
42. Singhose, W.E.; Seering, W.P.; Singer, N.C. Time-optimal negative input shapers. *J. Dyn. Sys. Meas. Control* **1997**, *119*, 198–205. [[CrossRef](#)]
43. Singhose, W.; Kim, D.; Kenison, M. Input shaping control of double-pendulum bridge crane oscillations. *J. Dyn. Sys. Meas. Control* **2008**, *130*, 034504. [[CrossRef](#)]
44. Hyde, J.M.; Seering, W.P. Inhibiting multiple mode vibration in controlled flexible systems. In Proceedings of the American Control Conference, Boston, MA, USA, 26–28 June 1991.
45. Cutforth, C.F.; Pao, L.Y. Adaptive input shaping for maneuvering flexible structures. *Automatica* **2004**, *40*, 685–693. [[CrossRef](#)]
46. Zhang, P.; Li, Y. Vibration control of flexible structure with multiple modes using input shaping. In Proceedings of the 2009 International Conference on Mechatronics and Automation, Changchun, China, 9–12 August 2009.
47. Sorensen, K.L.; Singhose, W.; Dickerson, S. A controller enabling precise positioning and sway reduction in bridge and gantry cranes. *Control Eng. Pract.* **2007**, *15*, 825–837. [[CrossRef](#)]
48. Goubej, M.; Martin, R.; Škarda, R.; Schlegel, M. Input Shaping Filters for the Control of Electrical Drive with Flexible Load. Website Name, 2009. Available online: <https://dspace5.zcu.cz/handle/11025/17198> (accessed on 31 October 2023).
49. Savitzky–Golay Filter. Available online: [https://en.wikipedia.org/wiki/Savitzky%E2%80%93Golay\\_filter](https://en.wikipedia.org/wiki/Savitzky%E2%80%93Golay_filter) (accessed on 31 October 2023).
50. Blackburn, D.; Singhose, W.; Kitchen, J.; Patrangenaru, V.; Lawrence, J.; Kamoi, T.; Taura, A. Command shaping for nonlinear crane dynamics. *J. Vib. Control* **2010**, *16*, 477–501. [[CrossRef](#)]

**Disclaimer/Publisher’s Note:** The statements, opinions and data contained in all publications are solely those of the individual author(s) and contributor(s) and not of MDPI and/or the editor(s). MDPI and/or the editor(s) disclaim responsibility for any injury to people or property resulting from any ideas, methods, instructions or products referred to in the content.